Journal of Alloys and Compounds 489 (2010) 482–487

Contents lists available at ScienceDirect

Journal of Alloys and Compounds

journal homepage: www.elsevier.com/locate/jallcom

Emissivity measurements on aeronautical alloys

L. del Campo[a,*], R.B. Pérez-Sáez[a,b,**], L. González-Fernández[a], X. Esquisabel[c], I. Fernández[c], P. González-Martín[d], M.J. Tello[a,b]

[a] Departamento de Física de la Materia Condensada, Facultad de Ciencia y Tecnología, Universidad del País Vasco, Barrio Sarriena s/n, 48940 Leioa, Bizkaia, Spain
[b] Instituto de Síntesis y Estudio de Materiales, Universidad del País Vasco, Apdo. 644, 48080 Bilbao, Spain
[c] Industria de Turbo Propulsores, S.A., Planta de Zamudio, Edificio 300, 48170 Zamudio, Bizkaia, Spain
[d] Industria de Turbo Propulsores, S.A., Parque empresarial San Fernando, Avda. Castilla 2, 28830 San Fernando de Henares, Madrid, Spain

ARTICLE INFO

Article history:
Received 16 July 2009
Received in revised form
15 September 2009
Accepted 16 September 2009
Available online 25 September 2009

Keywords:
High-temperature alloys
Thermodynamic properties
Infrared emissivity
Infrared spectroscopy

ABSTRACT

The emissivity of three Ni and Co based aeronautical alloys is analyzed in this paper. These alloys are employed in high temperature environments whenever good corrosion resistance, high temperature resistance and high strength are essential. Thus, apart from the aeronautical industry, these alloys are also used in other technological applications, as for example, aerospace, nuclear reactors, and tooling. The results in this paper extend the emissivity data for these alloys available in the literature. Emissivity dependence on the radiation wavelength (2–22 μm), sample temperature (200–650 °C) and emission angle (0–85°) has been investigated. In addition, the effect of surface finish and oxidation has also been taken into consideration. The data in this paper have several applications, as temperature measurement of a target by pyrometry, low observability of airplanes and thermal radiation heat transfer simulation in airplane nozzles or furnaces.

1. Introduction

The emissivity is a property which reveals how much radiation a given body emits as compared to a blackbody [1]. This magnitude is necessary in quite a lot of industrial and technological applications, as for example when taking into account thermal radiation heat transfer, especially in high temperature and vacuum environments. It is also essential when measuring the temperature of a target by radiometry (pyrometry). The emissivity is highly influenced by the surface state, thus it depends on surface roughness, oxidation, machining process, etc. Due to this influence, it is advisable to measure the emissivity of a sample in the operating conditions.

In the last years, there is an increasing requirement of the infrared emissivity of the alloys used in the aeronautical industry. The characterization of the emissivity of these alloys is crucial for several purposes, as for example, temperature measurement by pyrometry inside the airplane nozzle where a contact sensor is unfeasible, thermal radiation heat transfer in order to simulate temperature fields inside the nozzle, low observability of the airplanes to prevent missile detection, etc.

In order to obtain reliable emissivity data for aeronautical applications, three alloys are analyzed in this paper: Inconel 718, René 41 and Haynes 25. These Ni and Co based alloys are not only employed in the aeronautical industry. They are used in high temperature environments, whenever good oxidation and corrosion resistance and high mechanical strength are essential; for example, aerospace, nuclear reactors, and tooling applications. Inconel 718 is even utilized for cryogenic uses, as cryogenic storage tanks. The emissivity values can be also very usable in all these applications.

Ideally the emissivity should be measured under the service conditions of the required application. If this is not possible one should select adequate emissivity values from literature. Therefore the surface properties of the specimen have to be well-characterized as they influence the emissivity significantly. Any reference has been found where emissivity data for René 41 or Haynes 25 has been published. There are some references where the emissivity of the Inconel 718 has been measured [2–5], but only the total hemispherical emissivity or the spectral emissivity at a particular wavelength are given. Thus, Refs. [2,3] show that the total hemispherical emissivity rises with increasing surface roughness, temperature and oxidation state. Refs. [4,5] give some spectral emissivity values at 684.5 nm and 1.6 μm, respectively.

Some other references have been found for similar Ni and Co based alloys. For example, Ref. [6] shows indirect emissivity measurements (calculated using reflectivity data) for some Ni and Co

* Corresponding author. Present address: Conditions Extrêmes et Matériaux: Haute Température et Irradiation (CEMHTI), Centre National de la Recherche Scientifique (CNRS), Site Haute Température, 1D Av. de la Recherche Scientifique, 45071 Orléans Cedex 2, France. Tel.: +33 02 38 25 56 70; fax: +33 02 38 63 81 03.
** Corresponding author. Tel: +34 94 601 2655; fax: +34 94 601 3500.
E-mail addresses: leire.del-campo@cnrs-orleans.fr (L. del Campo), raul.perez@ehu.es (R.B. Pérez-Sáez).

0925-8388/$ – see front matter © 2009 Elsevier B.V. All rights reserved.
doi:10.1016/j.jallcom.2009.09.091

based alloys. Refs. [7,8] are related to a Thermophysical properties database where emissivity results for several compounds are found, for example Inconel 600, Inconel 601, and Inconel 625. Finally, some emissivity data for Inconel 600, Inconel X and Haynes 230 are given in Refs. [9–11].

In this paper, the available information for Inconel 718 is extended, and the first emissivity data for René 41 and Haynes 25 are presented. Emissivity dependence on the radiation wavelength (2–22 μm), sample temperature (200–650 °C) and emission angle (0–85°) has been investigated. Additionally, the effect of surface finish and oxidation has also been taken into consideration. The most widespread conditions have been accounted for in order to characterize the emissivity of these alloys the best possible.

2. Experimental

2.1. Samples

Three Ni and Co based alloys have been investigated: Inconel 718, René 41, and Haynes 25. Table 1 shows the components of the three alloys in weight percentage. As seen, the Inconel 718 and René 41 are Ni based, whereas the Haynes is Co based. It is remarkable that the three of them have a high Cr content.

Disk shaped samples, 2–3 mm thick cut from a 60 mm diameter rod have been used. The samples have been wire-cut by electrical discharge machining (EDM). Some of them have been additionally brushed, and certain also sandblasted. Thus, three surface finishes have been analyzed: wire-cut EDM, brushed, and sandblasted. The wire-cut EDM surfaces are dark coloured and look inhomogeneous due to a recast layer that is formed on the surface during the machining process. The brushing removes the recast layer, and smoothes the sample surface. This machining creates a surface profile with a strong unidirectional lay pattern. Finally, some of the brushed surfaces have been additionally sandblasted. This surface finish produces an isotropic surface profile.

Table 2 shows some roughness properties of the nine types of samples analyzed. The surface roughness average (R_a), average maximum height (R_z) and maximum height of the profile (R_t) have been measured for one sample of each type. As seen, the roughest samples are the wire-cut EDM. On the other hand, it is remarkable that the brushing and the sandblasting have produced very dissimilar surface topographies but with very similar roughness average parameters.

2.2. Emissivity measurements

The emissivity of the samples has been measured by means of a highly accurate homemade radiometer [12]. The samples are introduced in a vacuum sample chamber, and a resistance heater is used to heat them. The temperature of the sample surface is measured by bare K-type spot welded thermocouples, which are placed on the sample surface, out of the area viewed by the infrared detector. A PID temperature controller is used to control the sample temperature. The apparatus permits to obtain the angle dependence of the emissivity by tilting the sample and changing its polar angle (angle between the emission direction and the normal to the surface). The radiation emitted by the sample is detected by a Fourier transform infrared (FT-IR) spectrometer (Bruker IFS66v/S), and its radiance is compared with the radiance of a blackbody radiator. A simple comparison is not advisable because background radiation in the sample chamber and offset radiation inside the spectrometer have to be taken into account. Therefore, a shutter is placed in front of the blackbody, and a third measurement is performed. Finally, the three signals are used to get the sample spectral emissivity (ε) according to:

$$\varepsilon = \frac{FT[I_s - I_{sh}]}{FT[I_{bb} - I_{sh}]} \times \frac{L_{bb} - \varepsilon_{sh}L_{sh}}{L_s - L_{sur}} + \frac{\varepsilon_{sh}L_{sh} - L_{sur}}{L_s - L_{sur}} \quad (1)$$

where the subindices *s*, *bb*, *sh* and *sur* have been used for sample, blackbody, shutter and sample surroundings respectively. In the equation, *FT* means Fourier transform, I_i is used for *i*'s interferogram, and L_i for the blackbody radiance (Planck's equation) at temperature T_i. The measurement method is more precisely described in Refs. [12,13].

Before the emissivity measurements are performed, all the samples have been cleaned with acetone in an ultrasonic bath. Two K-type thermocouples have been spot welded in each sample, at two symmetric points 5 mm away from the centre. They do not disturb the radiation measurement as the area focalized at the detector is a 5 mm diameter disk centred at the sample. Before the samples are heated, the sample chamber is evacuated and a slightly reducing gas (N_2 + 5%H_2) is introduced. The H_2 is used to minimize sample oxidation. Thus, when the atmosphere inside the chamber is ready, the sample is heated till the desired temperature is achieved. Once the sample temperature is stable, the sample spectrum is acquired, next, the blackbody signal is measured, and then a third spectrum is obtained with the shutter placed in front of the blackbody. Finally, Eq. (1) is used to find the emissivity. The estimated uncertainty is less than 5%.

3. Results and discussion

The spectral normal emissivity has been measured for all the sample types shown in Table 2, for temperatures ranging from 200 to 650 °C, and for wavelengths between 2 and 22 μm. Two heating cycles have been measured for each sample. Furthermore, the spectral directional emissivity has been measured for sandblasted samples as a function of the emission angle, between the normal to the surface and 85°. Between 85° and 90° the emissivity can be extrapolated so that the hemispherical emissivity can be obtained. Additionally, the oxidation effect on the emissivity has also been studied for brushed samples.

Table 1
Chemical composition of Inconel 718, René 41 and Haynes 25 in weight percentage.

	Al	B	C	Co	Cr	Cu	Fe	Mn
Inconel 718	0.2–0.8	Max. 0.006	Max. 0.08	Max. 1	17–21	Max. 0.3	Balance (~20)	Max. 0.35
René 41	1.4–1.8	0.003–0.01	0.04–0.12	10–12	17.5–20		Max. 5	Max. 0.1
Haynes 25			0.05–0.15	Balance (~50)	19–21		Max. 3	1–2
	Mo	Nb	Ni	P	S	Si	Ti	W
Inconel 718	2.8–3.3	4.75–5.5	50–55	Max. 0.015	Max. 0.015	Max. 0.35	0.65–1.15	
René 41	9–10.5		Balance (~50)		Max. 0.015	Max. 0.5	3–3.3	
Haynes 25			9–11			Max. 0.4		14–16

Table 2
Summary of the samples with their surface roughness: roughness average (R_a), average maximum height (R_z), and maximum height of the profile (R_t).

Sample type	Alloy	Surface finish	R_a (μm)	R_z (μm)	R_t (μm)
1	Inconel 718	Brushed	1.3	8.2	9.9
2	Inconel 718	Sandblasted	1.6	8.0	–
3	Inconel 718	Wire-cut EDM	2.4	14.7	18.6
4	René 41	Brushed	1.5	10.1	13.0
5	René 41	Sandblasted	1.7	8.3	–
6	René 41	Wire-cut EDM	2.4	14.5	20.1
7	Haynes 25	Brushed	1.2	7.6	10.7
8	Haynes 25	Sandblasted	1.6	7.8	–
9	Haynes 25	Wire-cut EDM	2.7	16.4	19.9

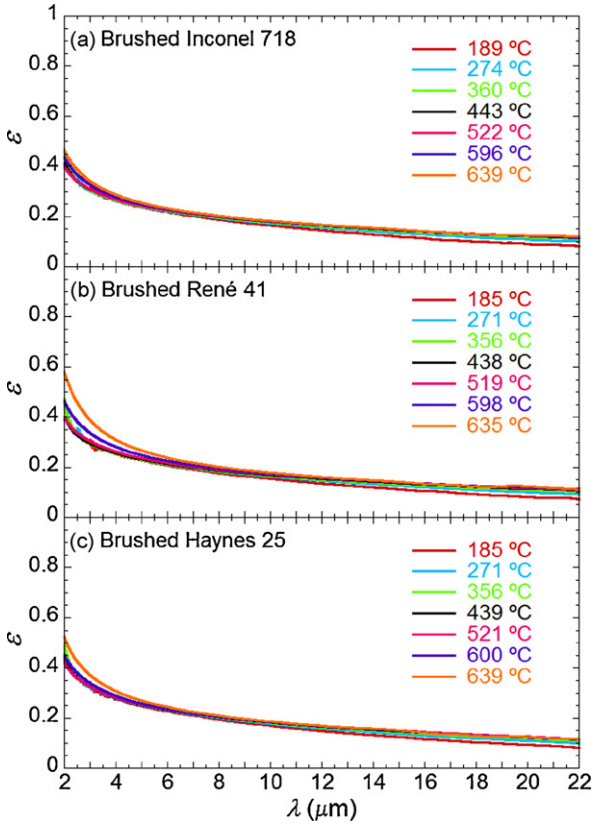

Fig. 1. Spectral normal emissivity (ε) of brushed samples as a function the wavelength (λ) for several temperatures: (a) Inconel 718 (sample type 1), (b) René 41 (sample type 4), and (c) Haynes 25 (sample type 7).

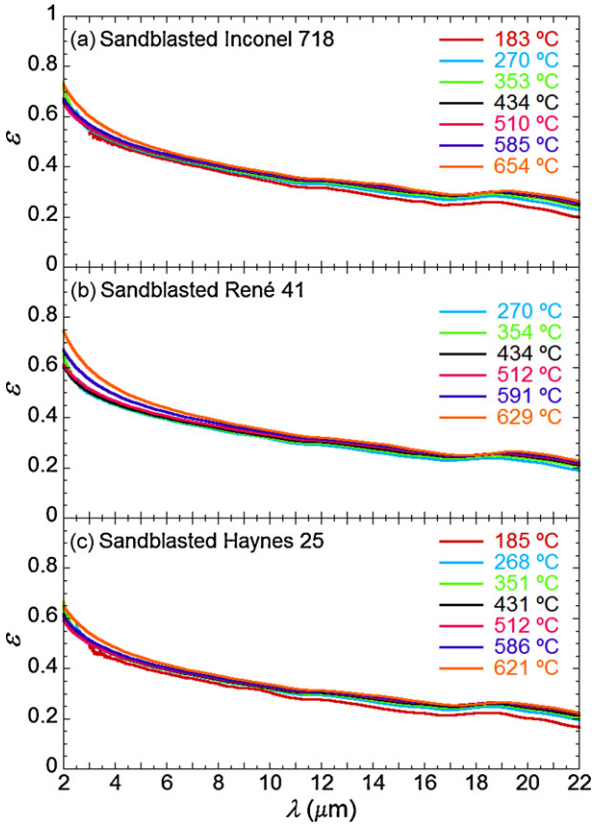

Fig. 2. Spectral normal emissivity (ε) of sandblasted samples as a function the wavelength (λ) for several temperatures: (a) Inconel 718 (sample type 2), (b) René 41 (sample type 5), and (c) Haynes 25 (sample type 8).

3.1. Dependence on temperature and wavelength

In Fig. 1, the measured spectral normal emissivity of brushed samples is shown as a function of the wavelength, for several sample temperatures. As seen, the temperature and wavelength dependence of the emissivity for the three brushed alloys is nearly the same, that is, it decreases with increasing wavelength, and a slight increase of the emissivity with temperature is observed at short and long wavelengths.

Nevertheless, the emissivity increase at short and long wavelengths has not the same cause, i.e., the emissivity at long wavelength returns to its initial value when cooling down, while at short wavelength, the increase in emissivity observed during the first cycle in maintained, that is, the emissivity does not return to its initial value when cooling down. Thus, the emissivity increase at long wavelengths is really related to a change in the emissive behaviour of the sample as the temperature changes, while the increase of the emissivity at short wavelength is related to a change in the sample surface during heating. As explained, the measurements have been performed in a slightly reducing atmosphere. Nevertheless, it is known that these Ni and Co alloys, as well as some stainless steels oxidize to some extent in reducing atmospheres. Actually, these alloys have a high Cr content, which oxidizes even in reducing atmospheres, as long as any small amount of oxygen is present. This is in accordance with the fact that the samples after heating show a bluish colour, which may be related to the chromium oxide formed on the sample surfaces. This is the reason that the emissivity increases with increasing temperature at short wavelength.

In Fig. 2 the emissivity spectra measured for the sandblasted samples are shown. As observed, the qualitative behaviour of the emissivity obtained for brushed and sandblasted samples is the same. The same emissivity increase is observed at short wavelengths, and accordingly, the sandblasted samples also look bluish after heating.

In Fig. 3 the same emissivity spectra are shown for wire-cut EDM surfaces. The recast layer contain some compounds that evaporate at high temperature and for that reason the emissivity varies during the first heating cycle, thus the results obtained during the second heating cycle are shown. As seen, the spectral dependence is basically the same as for brushed and sandblasted samples. However, the emissivity does not increase with temperature at short wavelength. This is probably due to the recast layer formed on the surface during the machining process, which inhibits further oxidation of the samples.

For the sake of a better visualisation of the variation of the spectral normal emissivity with the temperature, in Fig. 4 the emissivity of the nine types of samples is shown as a function of the temperature for several wavelengths (2.5 μm (Fig. 4a), 10 μm (Fig. 4b) and 20 μm (Fig. 4c)). For metallic samples, the emissivity usually increases with increasing temperature, but for these alloys, the emissivity nearly does not depend on the temperature for a broad spectral range in the studied temperature region.

3.2. Effect of surface finish and alloying element

The effect of surface finish and alloying element is already illustrated in Fig. 4 (Section 3.1). However, the comparison for the three alloys and the three surface finishes is better visualized in the graph in Fig. 5, where the emissivity spectra of the nine types of samples measured at $T \sim 515\,^{\circ}C$ are shown. The lowest emissivity is found for brushed samples and the highest for wire-cut EDM surfaces.

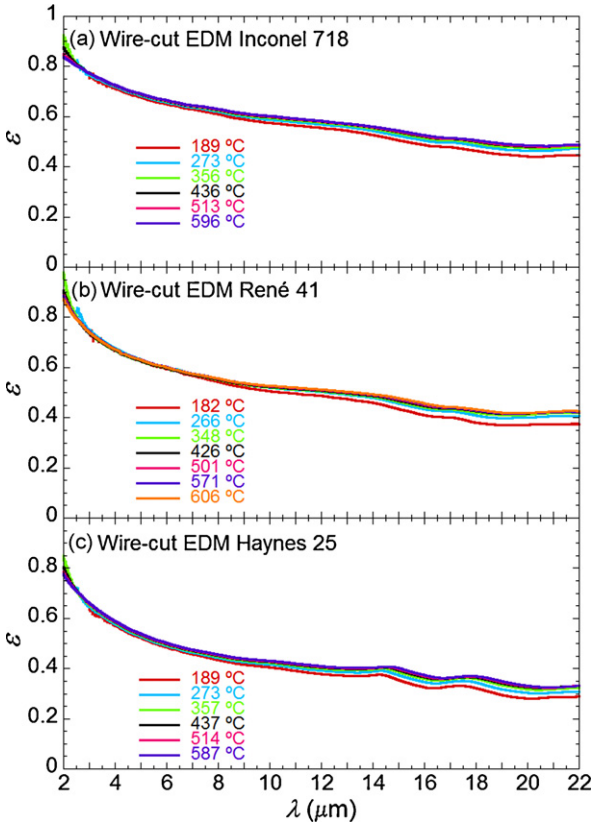

Fig. 3. Spectral normal emissivity (ε) of wire-cut EDM samples as a function the wavelength (λ) for several temperatures: (a) Inconel 718 (sample type 3), (b) René 41 (sample type 6), and (c) Haynes 25 (sample type 9).

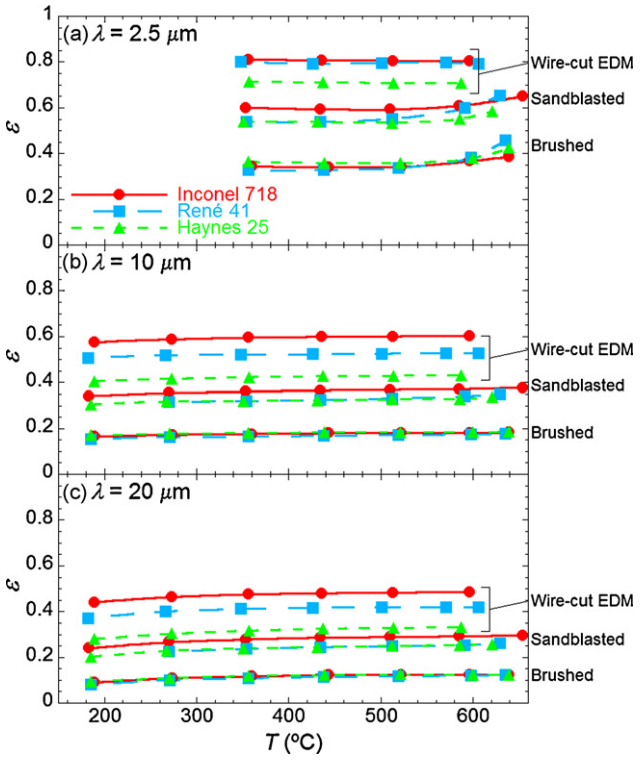

Fig. 4. Spectral normal emissivity (ε) of the nine types of samples in Table 2 plotted as a function of the temperature at wavelengths (λ): (a) $\lambda = 2.5\,\mu m$, (b) $\lambda = 10\,\mu m$, and (c) $\lambda = 20\,\mu m$.

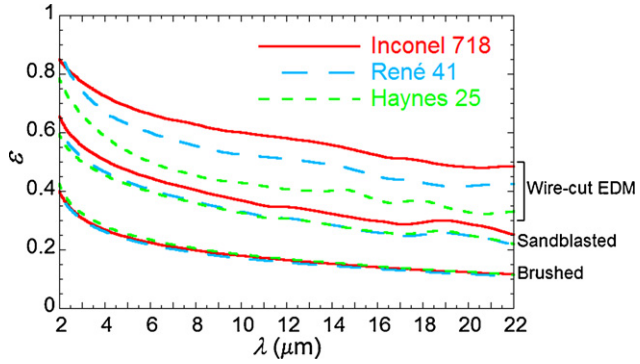

Fig. 5. Spectral normal emissivity (ε) of the nine types of samples in Table 2 as a function of the wavelength (λ) at a temperature of $T \sim 515\,^{\circ}C$.

On the other hand, it is remarkable that although the brushed and sandblasted samples have nearly the same roughness average values (see Table 2 in Section 2.1), their emissivity is quite different. This has to be related to the strong unidirectional lay pattern of the brushed surfaces, that is, the brushed samples have the roughness extended only in one direction (x direction), while sandblasted samples are rough in both directions (x and y direction), thus the latter are in fact rougher.

Besides, the emissivity of the brushed samples is nearly the same, while it is very different for wire-cut EDM surfaces. This is due to the recast layer on the wire-cut surfaces which may be different for each sample. Thus, the emissivity measured for the wire-cut EDM samples is strongly influenced by the recast layer formed during the machining process.

3.3. Dependence on the emission angle

The angular spectral emissivity has been measured for discrete angles between the normal and 85° using sandblasted samples. This surface finish has been chosen because of its isotropy, so that only the polar angle has to be taken into account. In Fig. 6 the angular emissivity of sandblasted samples measured at $T \sim 455\,^{\circ}C$ is displayed as a function of the emission angle, for several wavelengths. As seen, the three alloys exhibit a similar angular dependence. At short wavelengths, the emissivity nearly maintains constant till 60°, and then it starts to decrease until zero value is achieved at 90°. However, as the wavelength increases, the angular dependence becomes more "metallic-like", and above 10 μm, the emissivity increases from normal direction till it achieves a maximum at an angle close to 90°, and then abruptly goes to zero at 90°. The long wavelength behaviour is the expected one for a metallic sample, as predicted by the electromagnetic theory. Nevertheless, as the wavelength decreases and due to the surface texture, the angular dependence of the emissivity of the macroscopic surface differs from the one of microscopic surface, and the experimental results are different from the results predicted by the electromagnetic theory.

3.4. Effect of the oxidation

The alloys considered in this paper have a very good corrosion resistance. Emissivity measurements during in situ oxidation processes in air at 700 °C have been performed on brushed samples, but even after 20 h the emissivity variation due to oxidation was not so important, mainly at long wavelength. The results are shown in Fig. 7, where the emissivity spectra measured during the in situ oxidation process are shown for several oxidation times.

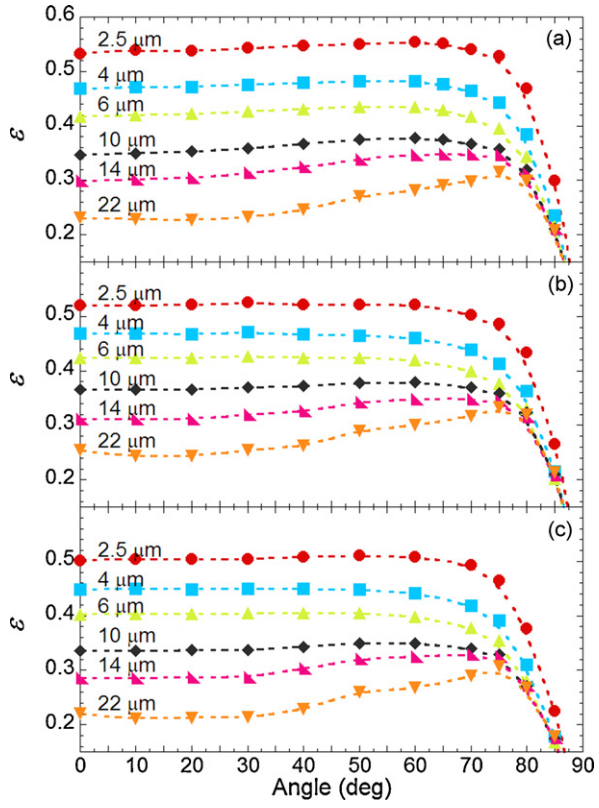

Fig. 6. Spectral directional emissivity (ε) of sandblasted samples as a function of the emission angle for several wavelengths at a temperature of T∼455 °C. (a) Inconel 718 (sample type 2), (b) René 41(sample type 5), and (c) Haynes 25 (sample type 8).

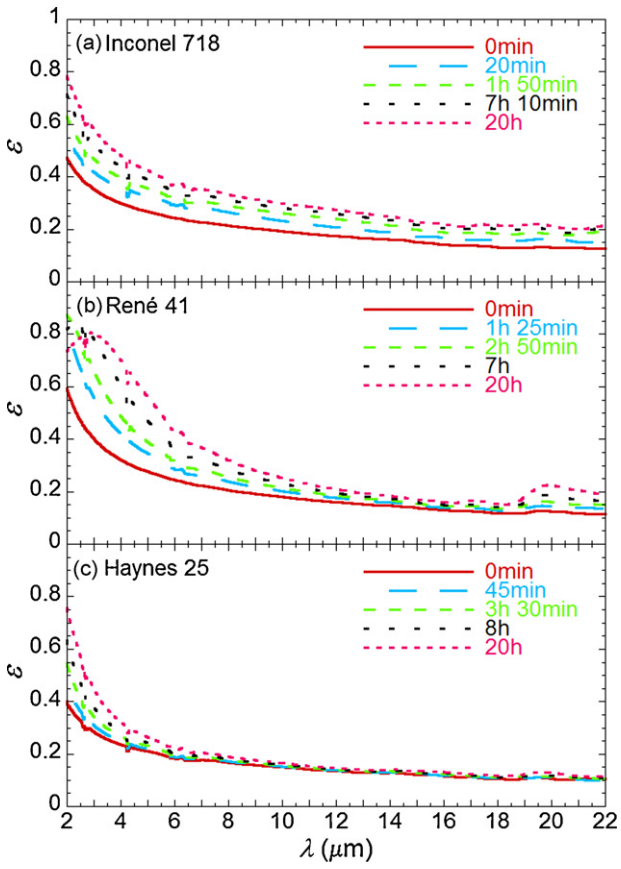

Fig. 7. Spectral normal emissivity (ε) of brushed samples for several oxidation times measured during an in situ oxidation process in air at 700 °C: (a) Inconel 718 (sample type 1), (b) René 41(sample type 4), and (c) Haynes 25 (sample type 7).

As seen, when the oxidation time increases, the emissivity rises. This fact is the expected since the emissivity of the oxides is usually higher than the emissivity of the metal. The less oxidation resistant alloy seems to be the René 41, while its emissivity is the one that most has changed after 20 h of oxidation process. This is also revealed in Figs. 1 and 2 (Section 3.1) where the emissivity increase with the temperature at short wavelength is more manifest for René 41 than for Inconel 718 and Haynes 25. Additionally, the maximum that appears in the emissivity at short wavelength (Fig. 7b) is due to radiation interferences in the oxide scale [14]. Even after 20 h of oxidation, the thickness of the oxide film formed on Inconel 718 and Haynes 25 is still too small for the interferences to appear. This also indicates that the oxide scale is thicker in the René 41 than in the other two samples.

The oxidation resistance of these alloys is considerably lowered when exposed to higher temperatures. Thus, a brushed Inconel 718 sample has been oxidized during 30 min in air at 900 °C using a separate furnace, and afterwards its emissivity has been measured as a function of the temperature. Fig. 8 shows the obtained normal emissivity spectra. On one hand, the interferencial extremes are already visible at short wavelength, thus the oxide scale has grown larger in 30 min at 900 °C than in 20 h at 700 °C. Additionally, the position of the maximum and minimum do not change as the temperature varies, consequently the sample is not further oxidizing. On the other hand, the oscillations observed in the emissivity at long wavelength are emission bands due to lattice vibrations of the oxide. It is clear that the phonon frequencies change with temperature and the bands broaden due to a rise in the damping parameter of the oscillators. An appropriate modelling of the emissivity could be performed to obtain the oxide thickness, as well as the optical indices and the frequencies of the normal modes [14–16].

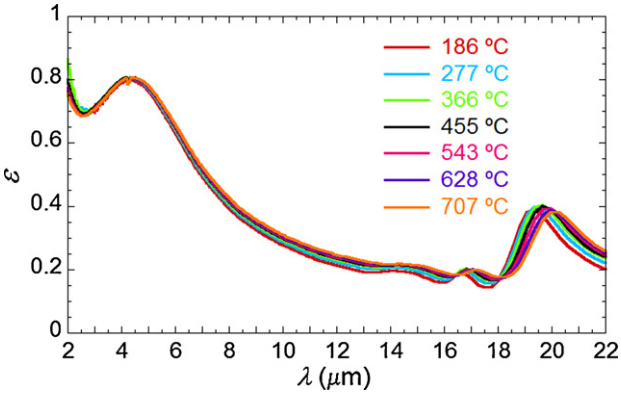

Fig. 8. Spectral normal emissivity (ε) of a brushed Inconel 718 sample pre-oxidized in air at 900 °C during 30 min, as a function of the wavelength (λ) and for several temperatures.

4. Conclusions

It has been found that the emissivity is nearly the same for the three studied Ni and Co alloys. In general terms, the emissivity decreases with increasing wavelength, and it is nearly independent of the temperature in the analyzed temperature range. The angular emissivity at short wavelengths maintains constant with increasing angle till 60° and then it becomes zero at 90°. In contrast, the angular emissivity at long wavelengths increases with increasing emission angle till it achieves a maximum, and then it drops to zero at 90°. Finally, oxidized samples have a higher emissivity, and inter-

ferential effects of the radiation due to the oxide scale have been found.

The spectral directional emissivity values given in this paper can be used to measure the temperature of a target by pyrometry. To do so, it is important to make sure that the alloy is not oxidized, because the emissivity can drastically change with oxidation. Finally, it is very important to identify the wavelength where the radiation sensor of the pyrometer detects, so as to use the emissivity at the correct wavelength.

These emissivity values can also be used to simulate thermal radiation heat transfer in an airplane nozzle or a furnace. If necessary, the total hemispherical emissivity can be calculated by integrating the spectral directional emissivity values given in this paper. More than 90% of the energy emitted by a body in the studied temperatures belongs to the spectral range between 2 and 12 μm, thus integration in this spectral range is enough to approximately obtain the total emissivity.

If the aim is to minimize infrared emission for low observability purposes, it is crucial to control the sample oxidation, and smooth surfaces are suitable. Thus it is advisable to smooth the metallic surfaces inside the nozzle, and an anti-oxidizing coating is appropriate. Among the three studied alloys, none is better or worse, as they have nearly the same emissivity.

Acknowledgements

This work has been carried out with the financial support of the SAIOTEK program (Project number S-PC08UN07) of the Basque Government and the "Universidad-Empresa" program (Project number UE06/01) of the University of the Basque Country in collaboration with "Industria de Turbopropulsores S.A.". L. González-Fernández acknowledges the Basque Government for their support through a Ph.D. fellowship. L. del Campo acknowledges the University of the Basque Country and the Basque Government for their support through Ph.D. and postdoctoral fellowships. She also gratefully thanks the "Radiative and Transport Properties of Materials" group of the CEMHTI (CNRS) laboratory at Orléans for the useful discussions during her postdoctoral stay.

References

[1] R. Siegel, J. Howell, Thermal Radiation Heat Transfer, fourth ed., Taylor & Francis, Washington, 2002.
[2] G. Tanda, M. Misale, J. Heat Trans. ASME 128 (2006) 302–306.
[3] G.A. Greene, C.C. Finfrock, T.F. Irvine Jr., Exp. Therm. Fluid Sci. 22 (2000) 145–153.
[4] G. Pottlacher, H. Hosaeus, B. Wilthan, E. Kaschnitz, A. Seifter, Thermochim. Acta 382 (2002) 255–267.
[5] S. Alaruri, L. Bianchini, A. Brewington, Opt. Lasers Eng. 30 (1998) 77–91.
[6] T. Makino, O. Sotokawa, Y. Iwata, Int. J. Thermophys. 9 (1988) 1121–1130.
[7] M. Kobayashi, M. Otsuki, H. Sakate, F. Sakuma, A. Ono, Int. J. Thermophys. 20 (1999) 289–298.
[8] M. Kobayashi, A. Ono, M. Otsuki, H. Sakate, F. Sakuma, Int. J. Thermophys. 20 (1999) 299–308.
[9] W. Bauer, H. Oertel, M. Rink, TEMPMEKO 2001—8th Symposium on Temperature and Thermal Measurement in Industry and Science, vol. 1, no. 30, Berlin, Germany, June 19–21, 2001, p. 306.
[10] W.J. O'Sullivan Jr., W.R. Wade, Theory and Apparatus for Measurement of Emissivity for Radiative Cooling of Hypersonic Aircraft with Data for Inconel and Inconel X, NACA Technical Note, 4121, 1957.
[11] J.R. Markham, K. Kinsella, R.M. Carangelo, C.R. Brouillette, M.D. Carangelo, P.E. Best, P.R. Solomon, Rev. Sci. Instrum. 64 (1993) 2515–2522.
[12] L. del Campo, R.B. Pérez-Sáez, X. Esquisabel, I. Fernández, M.J. Tello, Rev. Sci. Instrum. 77 (2006) 113111.
[13] R.B. Pérez-Sáez, L. del Campo, M.J. Tello, Int. J. Thermophys. 29 (2008) 1141–1155.
[14] L. del Campo, R.B. Pérez-Sáez, M.J. Tello, Corros. Sci. 50 (2008) 194–199.
[15] D. De Sousa Meneses, J.F. Brun, P. Echegut, P. Simon, Appl. Spectrosc. 58 (2004) 969–974.
[16] T. Iuchi, T. Furukawa, S. Wada, Appl. Opt. 42 (2003) 2317–2326.